

Bounding the average gate fidelity of composite channels using the unitarity

Arnaud Carignan-Dugas,¹ Joel J. Wallman,¹ and Joseph Emerson^{1,2}

¹*Institute for Quantum Computing and the Department of Applied Mathematics,
University of Waterloo, Waterloo, Ontario N2L 3G1, Canada*

²*Canadian Institute for Advanced Research, Toronto, Ontario M5G 1Z8, Canada*

There is currently a significant need for robust and efficient methods for characterizing quantum devices. While there has been significant progress in this direction, there remains a crucial need to precisely determine the strength and type of errors on individual gate operations, in order to assess and improve control as well as reliably bound the total error in a quantum circuit given some partial information about the errors on the components. In this work, we first provide an optimal bound on the total fidelity of a circuit in terms of component fidelities, which can be efficiently experimentally estimated via randomized benchmarking. We then derive a tighter bound that applies under additional information about the coherence of the error, namely, the unitarity, which can also be estimated via a related experimental protocol. This improved bound smoothly interpolates between the worst-case quadratic and best-case linear scaling for composite error channels. As an application we show how our analysis substantially improves the achievable precision on estimates of the infidelities of individual gates under interleaved randomized benchmarking, enabling greater precision for current experimental methods to assess and tune-up control over quantum gate operations.

I. INTRODUCTION

The output of a quantum computer will only be reliable if the total error in the whole computation is sufficiently small. This can be rigorously guaranteed if the error on the individual components (i.e., preparations, measurements and gate operations) is sufficiently small compared to the length of the computation. A very common experimental practice [1–12] for estimating errors on gate operations is randomized benchmarking (RB) of Clifford operations [13, 14]. The experimentally measured infidelities under RB experiments have very recently been shown to give a very precise estimate of the average gate fidelity (hereafter simply the fidelity) of an error channel to the identity,

$$F(\mathcal{E}) := \int d\psi \langle \psi | \mathcal{E}(|\psi\rangle\langle\psi|) | \psi \rangle \quad (1)$$

under very robust and experimentally realistic conditions [15–24], when expressed in a physical operational gauge [20–22, 25]¹, resolving the concern (that RB did not reliably measure a physically meaningful fidelity) raised in [26, 27].

An important practical application of RB is interleaved RB (IRB) [16], a now-standard approach for estimating infidelities on individual gates [1–4, 6, 8–12, 28–39], including gates that collectively generate universality [40–43]. However this approach is subject to a systematic error that can significantly limit the precision of the estimate and often goes unreported - a problem which we address below. As noted above, the average gate fidelity gives only very limited information about the error and error channels with the same fidelity on the component

gate operations can lead to dramatically different total error for a circuit composed from these gate operations. For example, the infidelity $r(\mathcal{E}) = 1 - F(\mathcal{E})$ grows linearly in the number of gates under purely stochastic errors (that is, errors that can be modeled by classical probabilities over different Pauli operators) and grows quadratically under purely unitary errors (that is, coherent errors due to small calibrations that are common in quantum control) in the limit of small infidelities [10]. However, realistic experimental errors are neither purely stochastic nor purely unitary, but rather some combination of the two. To adequately characterize quantum circuits, which are the result of multiple noisy operations, it is crucial to understand (and bound) how errors can accumulate given an intermediate level of coherence. In this paper, we study the impact of coherence on the fidelity of circuit constructions. An important application from our work is to provide a dramatic improvement to the achievable precision of IRB, enabling significantly more reliable experimental methods for assessing and tuning-up the individual gate operations required for quantum computing and other applications.

This paper is organized as follows. We first obtain strictly optimal upper- and lower-bounds on the total infidelity of the circuit for all parameter regimes when only the infidelities of the components are known. These bounds are saturated by unitary channels and so grow quadratically with the number of gates. Moreover, because our bounds are saturated, they cannot be improved without further knowledge about the errors. Because the worst-case growth of the infidelity is achieved by purely unitary channels, intuitively, quantifying how far an error channel is from purely unitary error should enable an improved bound. One such quantity is the unitarity. Thus our second contribution in this work is a proof that

¹ In Dugas et al, the physicality of the gauge is proven for $d = 2$, and conjectured otherwise.

the unitarity

$$u(\mathcal{E}) := \frac{d}{d-1} \int d\psi \operatorname{Tr} \mathcal{E}(\psi - \frac{1}{d}\mathbb{I})^2, \quad (2)$$

of the components, which can be estimated using a variant of RB [17, 24, 44] (URB), can be used to obtain a tighter bound on the total infidelity. This information enables a smooth interpolation between the quadratic growth of purely unitary errors and the linear scaling of purely stochastic errors. Including the unitarity to characterize circuits allows to quantitatively reason about an often omitted statement: elementary operations with low infidelity and highly coherent errors can rapidly compose to a worse circuit than a sequence of elementary operations with moderate infidelity but highly stochastic errors. Our bounds implicitly quantify how fast this can happen given the infidelity and unitarity of individual components. Our third contribution, noted above, goes the other way: from a composite error $\mathcal{E}_h \circ \mathcal{E}$, we bound the fidelity of one of its component \mathcal{E}_h . We demonstrate an immediate practical application of this result by providing a dramatically improved bound on the accuracy of the estimates of gate infidelities under interleaved RB [16]. This is done by substituting the estimate of the effective depolarizing constant of the individual interleaved gate $\hat{p} = p_{\text{IRB}}/p_{\text{RB}}$ by $\hat{p} = p_{\text{IRB}}p_{\text{RB}}/p_{\text{URB}}$, which requires a unitarity RB (URB) experiment. In the experiments reported in [45, 46], our estimator is used to rigorously bound the infidelity of individual quantum gates via eq. (42).

II. NOISY QUANTUM PROCESSES

Markovian quantum processes can be described by completely-positive and trace-preserving (CPTP) linear maps $\mathcal{E} : \mathbb{D}_d \rightarrow \mathbb{D}_d$ where \mathbb{D}_d is the set of density operators acting on \mathbb{C}^d , that is, the set of positive-semidefinite operators with unit trace. We denote quantum channels using single calligraphic capital Roman letters and the composition of channels by multiplication for brevity, so that $\mathcal{AB}(\rho) = \mathcal{A}[\mathcal{B}(\rho)]$. We also denote the composition of m channels $\mathcal{E}_1, \dots, \mathcal{E}_m$ by $\mathcal{E}_{1:m} = \mathcal{E}_1 \dots \mathcal{E}_m$.

Abstract quantum channels can be represented in many ways. In this paper, we will use the Kraus operator, χ -matrix and the Liouville (or transfer matrix) representations. The Kraus operator and χ -matrix representations of a quantum channel \mathcal{E} are

$$\mathcal{E}(\rho) = \sum_j A_j \rho A_j^\dagger = d \sum_{k,l \in \mathbb{Z}_{d^2}} \chi_{kl}^\mathcal{E} B_k \rho B_l^\dagger \quad (3)$$

respectively, where the A_j are the Kraus operators, $\mathbb{Z}_{d^2} = \{0, \dots, d^2 - 1\}$ and $\mathcal{B} = \{B_0 = \mathbb{I}_d/\sqrt{d}, B_1, \dots, B_{d^2-1}\}$ is a trace-orthonormal basis of $\mathbb{C}^{d \times d}$ satisfying $\langle B_j, B_k \rangle := \operatorname{Tr} B_j^\dagger B_k = \delta_{j,k}$. Note that we include the dimensional factor in the definition of the χ -matrix to be consistent

with the standard construction in terms of unnormalized Pauli operators.

The Kraus operators can be expanded as $A_j = \sum_{k \in \mathbb{Z}_{d^2}} \langle B_k, A_j \rangle B_k$ relative to \mathcal{B} . Making use of the phase freedom in the Kraus operators (that is, $A_j \rightarrow e^{i\theta_j} A_j$ gives the same quantum channel), we can set $\langle B_0, A_j \rangle \geq 0$ for all j . We can then expand the Kraus operators as

$$A_j = \sqrt{a_j d} \left(\cos(\alpha_j) B_0 + \sin(\alpha_j) \vec{v}_j \cdot \vec{\mathcal{B}} \right) \quad (4)$$

where $a_j d = \langle A_j, A_j \rangle$, $\vec{\mathcal{B}} = (B_1, \dots, B_{d^2-1})$, $\vec{v}_j \in \mathbb{C}^{d^2-1}$ with $\|\vec{v}_j\|_2 = 1$, and α_j can be chosen to be in $[0, \frac{\pi}{2}]$ by incorporating any phase into \vec{v}_j . Substituting this expansion into the Kraus operator decomposition and equating coefficients with the χ -matrix representation gives

$$\chi_{kl}^\mathcal{E} = \frac{1}{d} \sum_j \langle B_k, A_j \rangle \langle A_j, B_l \rangle, \quad (5)$$

and, in particular,

$$\chi_{00}^\mathcal{E} = \frac{1}{d^2} \sum_j |\operatorname{Tr} A_j|^2 = \sum_j a_j \cos^2(\alpha_j). \quad (6)$$

Applying the trace-preserving constraint with $\langle B_j, B_k \rangle = \delta_{j,k}$ gives

$$1 = \frac{1}{d} \operatorname{Tr} \sum_j A_j^\dagger A_j = \sum_j a_j, \quad (7)$$

which then implies

$$1 - \chi_{00}^\mathcal{E} = \sum_j a_j \sin^2(\alpha_j). \quad (8)$$

Alternatively, density matrices ρ and effects E (elements of positive-operator-valued measures) can be expanded with respect to \mathcal{B} as $\rho = \sum_j \langle B_j, \rho \rangle B_j$ and $E = \sum_j \langle B_j, E \rangle B_j$. The Liouville representations of ρ and E are the column vector $|\rho\rangle\rangle$ and row vector $\langle\langle E| = \langle\langle E|^\dagger$ of the corresponding expansion coefficients. The Born rule is then $\langle E, \rho \rangle = \langle\langle E| \rho \rangle\rangle$. The Liouville representation of a channel \mathcal{E} is the unique matrix \mathcal{E} such that $\mathcal{E}|\rho\rangle\rangle = |\mathcal{E}(\rho)\rangle\rangle$, which can be written as $\mathcal{E} = \sum_j |\mathcal{E}(B_j)\rangle\rangle \langle\langle B_j|$. With $B_0 = \mathbb{I}_d/\sqrt{d}$, the Liouville representation of any CPTP map can be expressed in block form as

$$\mathcal{E} = \begin{pmatrix} 1 & 0 \\ \mathcal{E}_n & \mathcal{E}_u \end{pmatrix} \quad (9)$$

where $\mathcal{E}_n \in \mathbb{C}^{d^2-1}$ is the non-unital vector and $\mathcal{E}_u \in \mathbb{C}^{(d^2-1) \times (d^2-1)}$ is the unital block. The unitarity and effective depolarizing constant can be written as

$$\begin{aligned} u(\mathcal{E}) &= \frac{\operatorname{Tr} \mathcal{E}_u^\dagger \mathcal{E}_u}{d^2 - 1} = \frac{\|\mathcal{E}_u\|_F^2}{d^2 - 1} \\ p(\mathcal{E}) &= \frac{\operatorname{Tr} \mathcal{E}_u}{d^2 - 1} \end{aligned} \quad (10)$$

| | F | r | p | χ_{00} |
|-------------|----------------------|----------------------|--------------------------|--------------------------------|
| F | F | $1 - r$ | $\frac{(d-1)p+1}{d}$ | $\frac{d\chi_{00}+1}{d+1}$ |
| r | $1 - F$ | r | $\frac{d-1}{d}(1-p)$ | $\frac{d}{d+1}(1-\chi_{00})$ |
| p | $\frac{dF-1}{d-1}$ | $1 - \frac{d}{d-1}r$ | p | $\frac{d^2\chi_{00}-1}{d^2-1}$ |
| χ_{00} | $\frac{(d+1)F-1}{d}$ | $1 - \frac{d+1}{d}r$ | $\frac{(d^2-1)p+1}{d^2}$ | χ_{00} |

TABLE I. Linear relations between the fidelity (F), the infidelity (r), the effective depolarizing constant (p), and χ_{00} .

with respect to the Liouville representation [17, 47].

The effective depolarizing constant $p(\mathcal{E})$ and χ_{00} are linear functions of the fidelity that can be more convenient to work with. The relations between the various linear functions of the fidelity used in this paper are tabulated in table I.

III. COMPOSITE INFIDELITIES IN TERMS OF COMPONENT INFIDELITIES

We now prove that unitary error processes lead to the fastest growth in the total infidelity of a circuit. In particular, we obtain strict bounds on the infidelity of a composite error process in terms of the infidelities of the components and show that the bounds are saturated by unitary processes for all even-dimensional systems.

We first obtain a bound on the infidelity of the composition of two channels that strictly improves on the corresponding bound of Ref. [47]. We also show that the improved bound is saturated for all values of the relevant variables. Therefore theorem 1 gives the optimal bounds on the infidelity of the composite in terms of only the infidelities of the components, and so obtaining a more precise estimate of the composite infidelity requires further information about the errors. We then obtain an upper bound on the infidelity of the composition of m channels that inherits the tightness of the bound for the composition of two channels.

We present the following bounds in terms of the χ matrix, though the results can be rewritten in terms of other linear functions of the infidelity using table I. For example, consider the composition of m noisy operations \mathcal{X}_i with equal infidelity, that is, $r(\mathcal{X}_i) = r$. Then by corollary 2 and table I, the total infidelity of the composite process is at most

$$r(\mathcal{X}_{1:m}) \leq m^2 r + O(m^4 r^2), \quad (11)$$

which exhibits the expected quadratic scaling with m . Moreover, this upper bound is saturated and so cannot

be improved without additional information about the errors.

Theorem 1. For any two quantum channels \mathcal{X} and \mathcal{Y} ,

$$\left| \chi_{00}^{\mathcal{X}\mathcal{Y}} - \chi_{00}^{\mathcal{X}}\chi_{00}^{\mathcal{Y}} - (1 - \chi_{00}^{\mathcal{X}})(1 - \chi_{00}^{\mathcal{Y}}) \right| \leq 2\sqrt{\chi_{00}^{\mathcal{X}}\chi_{00}^{\mathcal{Y}}(1 - \chi_{00}^{\mathcal{X}})(1 - \chi_{00}^{\mathcal{Y}})}. \quad (12)$$

Furthermore, for all even dimensions and all values of $\chi_{00}^{\mathcal{X}}$, $\chi_{00}^{\mathcal{Y}}$, there exists a pair of channels \mathcal{X} and \mathcal{Y} saturating both signs of the above inequality.

Proof. Let $\mathcal{X}(\rho) = \sum_j X_j \rho X_j^\dagger$ and $\mathcal{Y}(\rho) = \sum_j Y_j \rho Y_j^\dagger$ be Kraus operator decompositions of \mathcal{X} and \mathcal{Y} respectively. From eq. (4), we can expand the Kraus operators as

$$\begin{aligned} X_j &= \sqrt{x_j d} \left(\cos(\xi_j) B_1 + \sin(\xi_j) \vec{u}_j \cdot \vec{\mathcal{B}} \right) \\ Y_j &= \sqrt{y_j d} \left(\cos(\theta_j) B_1 + \sin(\theta_j) \vec{v}_j \cdot \vec{\mathcal{B}} \right) \end{aligned} \quad (13)$$

where $\vec{u}_j, \vec{v}_j \in \mathbb{C}^{d^2-1}$ are unit vectors and $\xi_j, \theta_j \in [0, \frac{\pi}{2}]$. Then a Kraus operator decomposition of $\mathcal{X}\mathcal{Y}$ is

$$\mathcal{X}\mathcal{Y}(\rho) = \sum_{j,k} X_j Y_k \rho Y_k^\dagger X_j^\dagger \quad (14)$$

and so, by eq. (6),

$$\chi_{00}^{\mathcal{X}\mathcal{Y}} = \sum_{j,k} x_j y_k |\cos \xi_j \cos \theta_k + \beta_{j,k} \sin \xi_j \sin \theta_k|^2, \quad (15)$$

where $\beta_{j,k} = \vec{u}_j \cdot \vec{v}_k$ and we have chosen the basis \mathcal{B} to be Hermitian so that $\text{Tr } B_j^\dagger B_k = \text{Tr } B_j B_k = \delta_{j,k}$. By the triangle and reverse-triangle inequalities,

$$|\alpha| - |\gamma| \leq |\alpha + \beta\gamma| \leq |\alpha| + |\gamma| \quad (16)$$

for any $\alpha, \beta, \gamma \in \mathbb{C}$ such that $|\beta| \leq 1$, which then implies

$$\left| |\alpha + \beta\gamma|^2 - |\alpha|^2 - |\gamma|^2 \right| \leq 2|\alpha\gamma|. \quad (17)$$

From eq. (6) and (8),

$$\begin{aligned} \sum_{j,k} x_j y_k |\cos(\xi_j) \cos(\theta_k)|^2 &= \chi_{00}^{\mathcal{X}} \chi_{00}^{\mathcal{Y}} \\ \sum_{j,k} x_j y_k |\sin(\xi_j) \sin(\theta_k)|^2 &= (1 - \chi_{00}^{\mathcal{X}})(1 - \chi_{00}^{\mathcal{Y}}), \end{aligned} \quad (18)$$

so by eq. (17),

$$\begin{aligned} \left| \chi_{00}^{\mathcal{X}\mathcal{Y}} - \chi_{00}^{\mathcal{X}}\chi_{00}^{\mathcal{Y}} - (1 - \chi_{00}^{\mathcal{X}})(1 - \chi_{00}^{\mathcal{Y}}) \right| \\ \leq \sum_{j,k} 2x_j y_k \cos(\xi_j) \cos(\theta_k) \sin(\xi_j) \sin(\theta_k), \end{aligned} \quad (19)$$

using $|\beta_{j,k}| \leq 1$ and the non-negativity of the trigonometric functions over $[0, \frac{\pi}{2}]$. Note that the above inequalities are saturated if and only if $\beta_{j,k} = \pm 1$.

By the Cauchy-Schwarz inequality with the fact that all the quantities are non-negative,

$$\begin{aligned} \sum_j x_j \sin(\xi_j) \cos(\xi_j) &\leq \sqrt{\sum_j x_j \sin^2(\xi_j)} \sqrt{\sum_j x_j \cos^2(\xi_j)} \\ &\leq \sqrt{(1 - \chi_{00}^{\mathcal{X}}) \chi_{00}^{\mathcal{X}}}, \end{aligned}$$

where the second line follows from eq. (6) and eq. (8). Applying this upper bound for \mathcal{X} and the corresponding one for \mathcal{Y} to eq. (19) gives the inequality in the theorem.

To see that both signs of the inequality are saturated for all values of $\chi_{00}^{\mathcal{X}}, \chi_{00}^{\mathcal{Y}}$ in even dimensions, let $\mathcal{X} = \mathcal{U}(\phi) \otimes \mathcal{I}_{d/2}$ and $\mathcal{Y} = \mathcal{U}(\theta) \otimes \mathcal{I}_{d/2}$ where

$$U(\phi) = e^{i\phi}|0\rangle\langle 0| + e^{-i\phi}|1\rangle\langle 1|. \quad (20)$$

By eq. (6), $\chi_{00}^{\mathcal{U}(\phi) \otimes \mathcal{I}_{d/2}} = \chi_{00}^{U(\phi)} = \cos^2 \phi$. As $\mathcal{X}\mathcal{Y} = \mathcal{U}(\phi + \theta) \otimes \mathcal{I}_{d/2}$, some trivial trigonometric manipulations give

$$\begin{aligned} \chi_{00}^{\mathcal{X}\mathcal{Y}} - \chi_{00}^{\mathcal{X}} \chi_{00}^{\mathcal{Y}} - (1 - \chi_{00}^{\mathcal{X}})(1 - \chi_{00}^{\mathcal{Y}}) \\ = -2 \cos \phi \sin \phi \cos \theta \sin \theta \\ = -2 \sqrt{\chi_{00}^{\mathcal{X}} \chi_{00}^{\mathcal{Y}} (1 - \chi_{00}^{\mathcal{X}})(1 - \chi_{00}^{\mathcal{Y}})} \text{sign}(\sin 2\phi \sin 2\theta), \end{aligned} \quad (21)$$

which saturates the lower bound if the sign function is positive and the upper bound if it is negative. \square

Corollary 2. For any m quantum channels \mathcal{X}_i such that

$$\sum_{i=1}^m \arccos \sqrt{\chi_{00}^{\mathcal{X}_i}} \leq \frac{\pi}{2}, \quad (22)$$

the χ_{00} element of the composite channel satisfies

$$\chi_{00}^{\mathcal{X}_{1:m}} \geq \cos^2 \left(\sum_{i=1}^m \arccos \sqrt{\chi_{00}^{\mathcal{X}_i}} \right). \quad (23)$$

Furthermore, this bound is saturated for all even dimensions and all values of the $\chi_{00}^{\mathcal{X}_i}$ satisfying eq. (22).

Proof. We can rewrite the lower bound in eq. (12) as

$$\sqrt{\chi_{00}^{\mathcal{X}\mathcal{Y}}} \geq \sqrt{\chi_{00}^{\mathcal{X}}} \sqrt{\chi_{00}^{\mathcal{Y}}} - \sqrt{1 - \chi_{00}^{\mathcal{X}}} \sqrt{1 - \chi_{00}^{\mathcal{Y}}}. \quad (24)$$

Writing $\sqrt{\chi_{00}} = \cos(\arccos \sqrt{\chi_{00}})$ and $\sqrt{1 - \chi_{00}} = \sin(\arccos \sqrt{\chi_{00}})$ and using standard trigonometric identities, the above becomes

$$\arccos \sqrt{\chi_{00}^{\mathcal{X}\mathcal{Y}}} \leq \arccos \sqrt{\chi_{00}^{\mathcal{X}}} + \arccos \sqrt{\chi_{00}^{\mathcal{Y}}}, \quad (25)$$

taking note to change the direction of the inequality when taking the arccos, which follows from eq. (22). By induction, we have

$$\arccos \left(\sqrt{\chi_{00}^{\mathcal{X}_{1:m}}} \right) \leq \sum_i \arccos \left(\sqrt{\chi_{00}^{\mathcal{X}_i}} \right) \quad (26)$$

for any set of m channels \mathcal{X}_i . Taking the cosine and squaring gives the bound in eq. (23). The saturation follows directly from the saturation of eq. (12). \square

A way to intuitively think about eq. (23) goes as follows: “the worst possible fidelity of a composition is obtained through a coherent (unitary) buildup”. Indeed, the trigonometric form of the inequality reflects this coherent nature.

IV. IMPROVED BOUNDS ON THE INFIDELITY USING THE UNITARITY

The bounds in theorem 1 and corollary 2 are tight for general channels if only the infidelity (or, equivalently, χ_{00}) is known. In particular, from eq. (11), the infidelity increases at most quadratically in m (to lowest order in r). However, the examples that saturate the bounds are all unitary channels. If, on the other hand, the error model is a depolarizing channel

$$\mathcal{D}_p(\rho) = p\rho + \frac{(1-p)}{d} \mathbb{I}_d, \quad (27)$$

or a Pauli channel (that is, a channel with a diagonal χ matrix with respect to the Pauli basis), then the infidelity increases at most linearly in m to lowest order, that is

$$r(\mathcal{X}_{1:m}) \leq mr + O(m^2 r^2). \quad (28)$$

The intermediate regime between Pauli errors and unitary errors can be quantified via the unitarity [17]. In particular, we define the (positive) coherence angle to be

$$\theta(\mathcal{E}) = \arccos \left(p(\mathcal{E}) / \sqrt{u(\mathcal{E})} \right). \quad (29)$$

As $u(\mathcal{E}) \leq 1$ with equality if and only if \mathcal{E} is unitary, $\theta(\mathcal{E}) \in [0, \arccos p(\mathcal{E})]$ and

$$\theta(\mathcal{E}) = \begin{cases} 0 & \text{iff } \mathcal{E} \text{ is depolarizing,} \\ O(r) & \text{iff } \mathcal{E} \text{ is Pauli,} \\ \arccos p(\mathcal{E}) = O(\sqrt{r}) & \text{iff } \mathcal{E} \text{ is unitary.} \end{cases} \quad (30)$$

That is, $\theta(\mathcal{E})$ quantifies the intermediate regime between Pauli and unitary errors for an isolated error process.

We now show that combining the coherence angle and the infidelity enables improved bounds on the growth of the infidelity. For example, for any m unitary channels, or for any m single qubit operations \mathcal{X}_i , with equal infidelity $r(\mathcal{X}_i) = r$ and coherence angles $\theta(\mathcal{X}_i) = \theta$, the total infidelity is at most

$$r(\mathcal{X}_{1:m}) \leq m \left(r - \frac{(d-1)\theta^2}{2d} \right) + m^2 \frac{(d-1)\theta^2}{2d} \quad (31)$$

plus higher-order terms in r and θ^2 by eq. (35). For Pauli errors, $\theta^2 = O(r^2)$, so we recover eq. (28). Conversely, for unitary errors $(d-1)\theta^2 = 2dr + O(r^2)$, so we recover eq. (11) in such regime. Moreover, the above bound is

saturated (to the appropriate order) in even dimensions by channels of the form

$$\mathcal{X}_i = \begin{pmatrix} 1 & 0 & 0 & 0 \\ 0 & \gamma \cos \theta(\mathcal{X}_i) & -\gamma \sin \theta(\mathcal{X}_i) & 0 \\ 0 & \gamma \sin \theta(\mathcal{X}_i) & \gamma \cos \theta(\mathcal{X}_i) & 0 \\ 0 & 0 & 0 & \lambda \end{pmatrix} \otimes \mathbb{I}_{d^2/2}. \quad (32)$$

These include the unital action of single qubit amplitude damping and dephasing channels combined with a unitary evolution around the dampening/dephasing axis. The unitary factor is parameterized by the coherence angle: $Z_\theta = \exp i2\theta Z$ (hence the ‘‘coherence’’ qualifier). In this sense, the coherence angle portays the allowed amount of rotation in Bloch space, as opposed to contractions (quantified by γ , λ in our saturation example) due to decoherent effects.

Theorems 3 and 4 result from more general matrix inequalities that we prove in appendix A. We apply the inequalities to the unital block of the Liouville representation from eq. (9), and substitute the expressions for the effective depolarizing constant and the unitarity from eq. (10). For theorem 4, we also use results from [48], which state that the maximal singular value of the unital block is upper-bounded by $\sqrt{\frac{d}{2}}$ for general channels and 1 for unital channels.

Theorem 3. *For any two quantum channels \mathcal{X} and \mathcal{Y} ,*

$$\cos[\theta(\mathcal{X}) + \theta(\mathcal{Y})] \leq \frac{p(\mathcal{X}\mathcal{Y})}{\sqrt{u(\mathcal{X})u(\mathcal{Y})}} \leq \cos[\theta(\mathcal{X}) - \theta(\mathcal{Y})]. \quad (33)$$

In other words, the leeway in the effective depolarizing constant of a composition $\mathcal{X}\mathcal{Y}$ is limited by constructive and destructive coherent effects. For longer compositions, we have:

Theorem 4. *For any m channels \mathcal{X}_i with $p(\mathcal{X}_i) = p$, $u(\mathcal{X}_i) = u$, the effective depolarizing constant of the composite channel satisfies*

$$|p(\mathcal{X}_{1:m}) - p^m| \leq \sqrt{\frac{d}{2}} \binom{m}{2} u \sin^2(\theta). \quad (34)$$

Furthermore, if the \mathcal{X}_i are unital channels, the bound can be improved to

$$|p(\mathcal{X}_{1:m}) - p^m| \leq \binom{m}{2} u \sin^2(\theta). \quad (35)$$

Notice that the binomial factor – which indicates a quadratic behavior in m – demonstrates that the effective depolarizing constant of a large composition, $p(\mathcal{X}_{1:m})$, can quickly differ from p^m . This difference grows quicker with the coherence angle, which can be tied to coherent effects through eq. (32).

The bounds in theorem 3 can be made even tighter if one of the channels is guaranteed to be Pauli.

Theorem 5. *Consider a Pauli channel \mathcal{X} and any quantum channel \mathcal{Y} . Then, the composite infidelity is essentially linear in the individual infidelities $r(\mathcal{X})$ and $r(\mathcal{Y})$:*

$$r(\mathcal{X}\mathcal{Y}) = r(\mathcal{X}) + r(\mathcal{Y}) + O(r(\mathcal{X})r(\mathcal{Y})). \quad (36)$$

This bound is to be contrasted with the naive usage of theorem 3:

$$\begin{aligned} r(\mathcal{X}\mathcal{Y}) &= r(\mathcal{X}) + r(\mathcal{Y}) + O(\theta(\mathcal{X})\theta(\mathcal{Y})) \quad (\text{theorem 3}) \\ &= r(\mathcal{X}) + r(\mathcal{Y}) + O(r(\mathcal{X})\sqrt{r(\mathcal{Y})}). \quad (\text{eq. (30)}) \end{aligned}$$

The improvement can be easily shown as follow. The infidelity is invariant under unitary conjugation $r(\mathcal{X}\mathcal{Y}) = r(\mathcal{U}\mathcal{X}\mathcal{Y}\mathcal{U}^\dagger)$ or convex combination of thereof. In particular, it is invariant under a Pauli twirl. Since \mathcal{X} is a Pauli channel, it commutes with Pauli unitaries, and the twirl gets effectively performed on \mathcal{Y} , which becomes a Pauli channel $\mathcal{Y}_{\text{Pauli}}$ with low coherence angle $\theta(\mathcal{Y}_{\text{Pauli}}) = O(r(\mathcal{Y}))$ (see eq. (30)). From there we can apply theorem 3.

Theorems 3 and 4 implicitly suggest that using the coherence angle (rather than the infidelity) as the objective function² for optimizing operations would strongly tighten eventual assertions about the fidelity of circuit constructions.

V. APPLICATION: INTERLEAVED RB

The fidelity extracted from standard RB experiments typically characterizes the average error over a gate set \mathcal{G} , defined as

$$\mathcal{E} := |\mathcal{G}|^{-1} \sum_{g \in \mathcal{G}} \mathcal{E}_g. \quad (37)$$

However, one might only care about the fidelity $F(\mathcal{E}_h)$ attached to a specific gate of interest $h \in \mathcal{G}$, such as one of the generators required for universal quantum computing. The interleaved RB protocol (IRB) [16] yields a fidelity estimate of $\mathcal{E}_h \mathcal{E}^3$, the composition between the single gate error and the gate set error, which provides bounds on the desired value $F(\mathcal{E}_h)$. An issue with this approach is that these bounds generally have a wide range, since possible coherent effects cannot be ignored. This issue is illustrated by the results of two simulations of interleaved RB experiments, plotted in fig. 1. In both scenarios, the fidelity of the gate error and of the composed gate were fixed at $F(\mathcal{E}) = 0.9975$ and $F(\mathcal{E}_h \mathcal{E}) = 0.9960$ respectively, hence leading to the same single gate fidelity estimate. In the first case, the interleaved gate h is unitary with high fidelity ($F(\mathcal{E}_h) = 0.9991$), whereas in the

² A more stable choice would be $\sin^2(\theta)$.

³ For the sake of simplicity, we assume that the protocols all provide fidelity estimates defined with respect to the same (or very close) ideal representation of gates.

second case the error is depolarizing, with a lower fidelity ($F(\mathcal{E}_h) = 0.9975$). This example illustrates how interleaved RB, without a measure of unitarity, can only provide a loose estimate of the infidelity of an individual gate.

More generally, rearranging the bound in theorem 1 to isolate $\chi_{00}^{\mathcal{Y}}$ gives

$$\left| \chi_{00}^{\mathcal{Y}} - \chi_{00}^{\mathcal{X}\mathcal{Y}} \chi_{00}^{\mathcal{X}} - (1 - \chi_{00}^{\mathcal{X}\mathcal{Y}})(1 - \chi_{00}^{\mathcal{X}}) \right| \leq 2\sqrt{\chi_{00}^{\mathcal{X}\mathcal{Y}} \chi_{00}^{\mathcal{X}} (1 - \chi_{00}^{\mathcal{X}\mathcal{Y}})(1 - \chi_{00}^{\mathcal{X}})}. \quad (38)$$

Moreover, this bound cannot be improved without further information. Now suppose that $r(\mathcal{E}_h\mathcal{E}) \approx 2r(\mathcal{E})$, so that the uncertainty of $r(\mathcal{E}_h)$, obtained via eq. (38) and table I is

$$\Delta r(\mathcal{E}_h) \approx 4\sqrt{2}r(\mathcal{E}). \quad (39)$$

While this bound does give an estimate of the infidelity, this estimate is comparable to the following naive estimate that requires no additional experiment. As the fidelity, and hence the infidelity, is a linear function of \mathcal{E} we have

$$r(\mathcal{E}) = |\mathcal{G}|^{-1} \sum_{g \in \mathcal{G}} r(\mathcal{E}_g) \quad (40)$$

which, since $r(\mathcal{E})$ is non-negative for any channel \mathcal{E} , implies

$$r(\mathcal{E}_h) \leq |\mathcal{G}|r(\mathcal{E}) \quad (41)$$

for any $h \in \mathcal{G}$. (Note also that this bound can be heuristically improved by identifying sets of gates that are expected to have comparable error.) When \mathcal{G} is chosen to be the 12-element subgroup of the Clifford group that forms a unitary 2-design, the naive bound is, at the very worst, a factor of $3/\sqrt{2}$ worse than the bound from interleaved benchmarking and requires no additional statistical analysis or data collection.

However, if the error channels were guaranteed to be depolarizing, $F(\mathcal{E}_h)$ could be exactly estimated from an interleaved RB experiment. In general, we can use our knowledge of the unitarity of \mathcal{E} – which can be obtained from a URB experiment⁴ – to quantify how close the error model is to depolarizing noise. From theorem 3, we then have the following bounds, which can be orders of magnitude tighter as illustrated in fig. 2.

Corollary 6. *For any two quantum channels \mathcal{E}_h and \mathcal{E} ,*

$$\left| p(\mathcal{E}_h) - \frac{p(\mathcal{E}_h\mathcal{E})p(\mathcal{E})}{u(\mathcal{E})} \right| \leq \sqrt{1 - \frac{p(\mathcal{E})^2}{u(\mathcal{E})}} \sqrt{1 - \frac{p(\mathcal{E}_h\mathcal{E})^2}{u(\mathcal{E})}}. \quad (42)$$

⁴ The current analysis of URB is done under a gate-independent noise approximation.

Notice that this new estimate of $p(\mathcal{E}_h)$ is an amalgam of three experiments: standard RB, IRB and unitarity RB. A recommended experimental practice would be, for instance [46]:

- Perform standard RB over the Clifford group. Estimate the resulting decay parameter $p(\mathcal{E})$, where \mathcal{E} is tied to the average error over the Clifford group.
- Perform unitarity RB over the Clifford group. Estimate the resulting decay parameter, which corresponds to the unitarity $u(\mathcal{E})$.
- Perform IRB with the Clifford group as randomizing set and h as ideal gate of interest. Estimate the resulting decay constant $p(\mathcal{E}_h\mathcal{E})$, where \mathcal{E}_h is the error map attached to h .
- Use eq. (42) to bound $p(\mathcal{E}_h)$, and use table I to convert it to the fidelity (or infidelity).

Recall that in the depolarizing case $u(\mathcal{E}) = p(\mathcal{E})^2$, for which eq. (42) reduces to the familiar equality $p(\mathcal{E}_h) = p(\mathcal{E}_h\mathcal{E})/p(\mathcal{E})^5$. In fact, the equality remains true up to order $r(\mathcal{E})^2$ in the more general case of stochastic Pauli errors, as demonstrated in theorem 5. Treating the infidelity as a linear quantity under composition is a very common assumption stemming from a classical probabilistic view of error accumulation. To take another example of a linear manipulation, the infidelity per pulse (or infidelity per primitive gate) is often obtained by implicitly dividing the infidelity of a set of composite gates by the average number of pulses used to generate them. These are not bad estimates only if the error is mostly stochastic. This might be a valid presumption since many error mechanisms are naturally stochastic, but is certainly not a trivial one, since coherent effects also commonly arise from faulty control. The present paper offers a means to avoid the often unrealistic stochasticity assumption by explicitly providing a confidence interval based on experimental estimates of the unitarity. To illustrate the idea, in fig. 3 we applied our bounds on various experimental results [1–4, 8–12] and varied the value of the unitarity.

VI. SUMMARY AND OUTLOOK

In this paper, we have studied the impact of coherent errors on the fidelity of quantum circuits. We first demonstrate why coherent errors are a serious concern: a coherent composition of unitary quantum channels results in the fastest decay of the fidelity. In this case, the infidelity grows quadratically in the number of gates, in

⁵ In the interleaved RB lingo, this relation is often expressed as $p(\mathcal{E}_h) = p_{\text{IRB}}/p_{\text{RB}}$, where \mathcal{E}_h is the error attached to the interleaved gate.

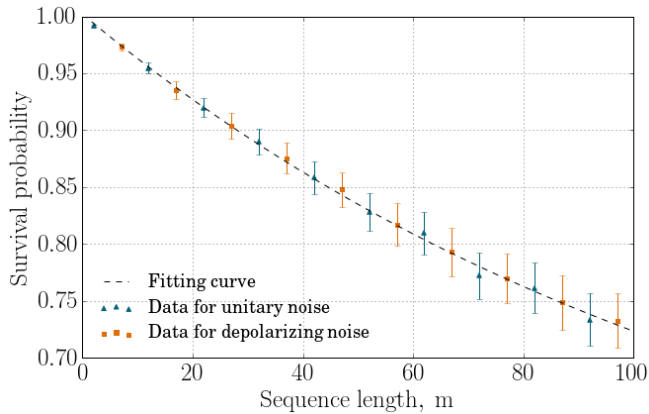


FIG. 1. (Color online) The average survival probability, $p_{\text{surv.}}(m) = |\mathcal{G}|^{-m} \sum_i \langle 0 | \mathcal{S}_m^{(i)} (|0\rangle\langle 0|) |0\rangle$ over all sequences $\mathcal{S}_m^{(i)}$ of length m , as a function of the sequence length for two simulated interleaved RB experiments (see Ref. [16] for more details) with two different individual gate errors \mathcal{E}_h , but a common average error \mathcal{E} with fidelity 0.9975. Orange squares represent an error model with high fidelity ($F(\mathcal{E}_h) = 0.9991$) that interacts coherently with \mathcal{E} . Blue triangles represent an error model with lower fidelity ($F(\mathcal{E}_h) = 0.9975$), but that is purely stochastic. See section V for more details.

contrast with the linear growth for stochastic Pauli channels. The disparity between these two regimes means that the characterization of the gate fidelities alone only allows to formulate weak statements about the fidelity of more elaborate circuit constructions.

Hence, in order to characterize circuits more precisely, we introduced a coherence angle—which corresponds to a rotation angle on the Bloch space, as opposed to a contraction (see eq. (29))—which enables a tighter bound on the total error in a quantum circuit in terms of robustly estimable quantities that smoothly interpolates between the linear and quadratic regimes.

Our new bound can be used upside-down: from the fidelity of a small circuit construction, we can bound the fidelity of one of its elements. As an immediate application, we demonstrated that this bound substantially improves the estimates of individual gate fidelities from interleaved randomized benchmarking, which, in the absence of the improved bound, are comparable to the naive bound obtained by noting that the infidelity from standard RB is the average of the infidelities of the individual gates. The practicality of corollary 6 relies on the implicit assumption that the unitarity obtained from RB as well as the average gate fidelities are resulting from closely related gauges[20–22]. An open problem would be to relax this assumption by connecting more rigorously the interpretations of different RB experiments.

Acknowledgments — This research was supported by the U.S. Army Research Office through grant W911NF-14-1-0103, CIFAR, the Government of Ontario, and the Government of Canada through CFREF, NSERC and Industry Canada.

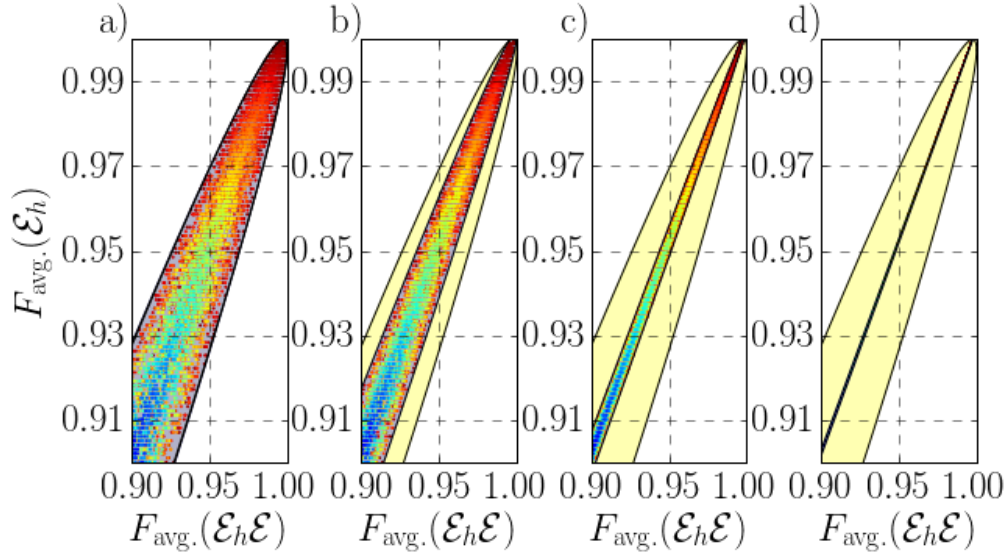


FIG. 2. (Color online) Bounds on the fidelity $F(\mathcal{E}_h)$ of an individual gate h as a function of the composite $F(\mathcal{E}_h\mathcal{E})$ with $F(\mathcal{E})$ fixed and varying $u(\mathcal{E})$: a) $u(\mathcal{E}) = 1.00000$, b) $u(\mathcal{E}) = 0.99300$, c) $u(\mathcal{E}) = 0.99030$, d) $u(\mathcal{E}) = 0.99003 \approx p(\mathcal{E})^2$. The numerical data points correspond to the values $F(\mathcal{E}_h)$ and $F(\mathcal{E}_h\mathcal{E})$ for randomly-generated channels $\{\mathcal{E}_h, \mathcal{E}\}$ satisfying $F(\mathcal{E}) = 0.9975$ and with the appropriate value of $u(\mathcal{E})$. As illustrated by the color, the unitarity $u(\mathcal{E}_h)$ is minimal in the center of the shaded region and maximal when the data points approach our bound.

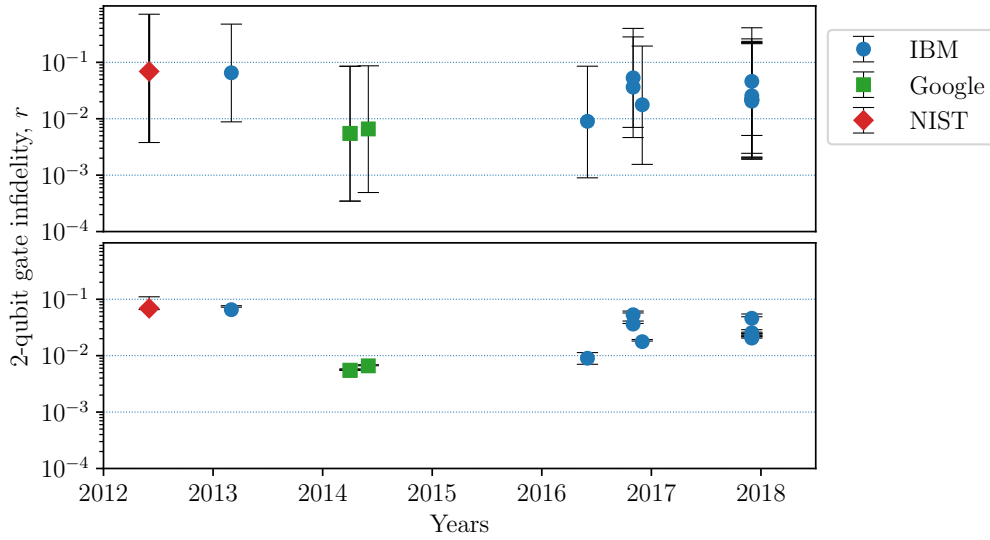


FIG. 3. (Color online) Bounds on various 2-qubit gate infidelities $r(\mathcal{E}_h)$ based on various experimental data [1–4, 8–12]. The time refers to the dates of submission. The top plot uses eq. (42) with a maximal coherence angle $\theta(\mathcal{E})$, which yields in bounds spanning up to two orders of magnitude. The bottom plot assumes a purely stochastic error model, by which we mean that $u(\mathcal{E}) \approx p(\mathcal{E})^2$. For every data point, some statistical error is taken into account, hence the non-zero error bars in the bottom plot.

Appendix A: Matrix inequalities on the real field

We define the coherence angle of a matrix $M \in \mathbb{R}^{d \times d}$ to be

$$\theta(M) := \arccos \left(\frac{\text{Tr } M}{\sqrt{d} \|M\|_F} \right) \in [0, \pi]. \quad (\text{A1})$$

Theorem 7. For any nonzero $M_1, M_2 \in \mathbb{R}^{d \times d}$,

$$\cos[\theta(M_1) + \theta(M_2)] \leq \frac{\text{Tr } M_1 M_2}{\|M_1\|_F \|M_2\|_F} \leq \cos[\theta(M_1) - \theta(M_2)]. \quad (\text{A2})$$

Moreover, both bounds are saturated for all values of $\|M_1\|_F$, $\|M_2\|_F$, $\theta(M_1)$, and $\theta(M_2)$ in even dimensions.

Proof. By the Cauchy-Schwarz inequality,

$$|\text{Tr } AB|^2 = \left(\sum_{i,j} A_{i,j} B_{j,i} \right)^2 \leq \left(\sum_{i,j} A_{i,j}^2 \right) \left(\sum_{i,j} B_{j,i}^2 \right) = (\text{Tr } A^\dagger A) (\text{Tr } B^\dagger B) = \|A\|_F^2 \|B\|_F^2. \quad (\text{A3})$$

Setting $D_i := \frac{\text{Tr } M_i}{d} \mathbb{I}_d$ for $i = 1, 2$,

$$\begin{aligned} \|M_i - D_i\|_F &= \sqrt{\text{Tr}(M_i^\dagger M_i - M_i^\dagger D_i - D_i^\dagger M_i + D_i^\dagger D_i)} \\ &= \sqrt{\|M_i\|_F^2 - d^{-1} (\text{Tr } M_i)^2} \\ &= \|M_i\|_F \sqrt{1 - \cos^2 \theta(M)} \\ &= \|M_i\|_F \sin \theta(M) \end{aligned} \quad (\text{A4})$$

using $\text{Tr } M^\dagger = \text{Tr } M$, which holds for $M \in \mathbb{R}^{d \times d}$. Setting $A = M_1 - D_1$ and $B = M_2 - D_2$ in eq. (A3) and using eq. (A4) gives

$$|\text{Tr}(M_1 - D_1)(M_2 - D_2)| \leq \|M_1\|_F \|M_2\|_F \sin \theta(M_1) \sin \theta(M_2). \quad (\text{A5})$$

Using eq. (A1) on the left-hand side gives

$$\begin{aligned} |\text{Tr}(M_1 - D_1)(M_2 - D_2)| &= |\text{Tr } M_1 M_2 - d^{-1} \text{Tr } M_1 \text{Tr } M_2| \\ &= |\text{Tr } M_1 M_2 - \|M_1\|_F \|M_2\|_F \cos[\theta(M_1)] \cos[\theta(M_2)]|. \end{aligned} \quad (\text{A6})$$

Combining eqs. (A5) and (A6) with the identity $\cos(a \pm b) = \cos(a) \cos(b) \mp \sin(a) \sin(b)$ gives both desired inequalities. For even d , the bounds of eq. (A2) are saturated by

$$\frac{\|M_i\|_F}{\sqrt{d}} \begin{pmatrix} \cos \theta(M_i) & -\sin \theta(M_i) \\ \sin \theta(M_i) & \cos \theta(M_i) \end{pmatrix} \otimes \mathbb{I}_{\frac{d}{2}}. \quad (\text{A7})$$

□

We can generalize the lower bound of eq. (A2) to matrix products $M_{1:m} := M_1 M_2 \cdots M_m$.

Theorem 8. Let $M_1, \dots, M_m \in \mathbb{R}^{d \times d}$ be such that for all j , $\theta(M_j) = \theta$, $\frac{\text{Tr}(M_j)}{d} = p \leq 1$, $\frac{\|M_j\|_F^2}{d} = u \leq 1$, and $\|M_{1:j}\|_2 \leq \sigma_{\max}$. Then,

$$\left| \frac{\text{Tr } M_{1:m}}{d} - p^m \right| \leq \sigma_{\max} \left(\frac{1 - mp^{m-1} - (m-1)p^m}{(1-p)^2} \right) u \sin^2(\theta) \leq \sigma_{\max} \binom{m}{2} u \sin^2(\theta). \quad (\text{A8})$$

Proof. Let $D := p\mathbb{I}_d$, and $M_j = D + \Delta_j$. Using a telescoping expansion twice gives

$$\begin{aligned} M_{1:m} - D^m &= \sum_{i=1}^m M_{1:i-1} (M_i - D) D^{m-i} \\ &= \sum_{i=1}^m [D^{i-1} + \sum_{j=1}^{i-1} M_{1:j-1} \Delta_j D^{i-1-j}] \Delta_i D^{m-i}. \end{aligned} \quad (\text{A9})$$

Taking the trace of each side and using $\text{Tr } \Delta_j = 0$ gives

$$\text{Tr } M_{1:m} - dp^m = \sum_{i=1}^m \sum_{j=1}^{i-1} p^{m-j-1} \text{Tr } M_{1:j-1} \Delta_j \Delta_i . \quad (\text{A10})$$

Therefore

$$\begin{aligned} |\text{Tr } M_{1:m} - dp^m| &= \left| \sum_{i=1}^m \sum_{j=1}^{i-1} p^{m-j-1} \text{Tr } M_{1:j-1} \Delta_j \Delta_i \right| \\ &\leq \sum_{i=1}^m \sum_{j=1}^{i-1} p^{m-j-1} |\text{Tr } M_{1:j-1} \Delta_j \Delta_i| \quad (\Delta \text{ inequality}) \\ &\leq \sum_{i=1}^m \sum_{j=1}^{i-1} p^{m-j-1} \|M_{1:j-1} \Delta_j\|_F \|\Delta_i\|_F \quad (\text{Cauchy-Schwarz inequality}) \\ &\leq \sum_{i=1}^m \sum_{j=1}^{i-1} p^{m-j-1} \sigma_{\max} \|\Delta_j\|_F \|\Delta_i\|_F \quad ([49, \text{Prop. 9.3.6}]) \\ &= \sigma_{\max} du \sin^2(\theta) \sum_{i=1}^m \sum_{j=1}^{i-1} p^{m-j-1} , \quad (\text{A11}) \end{aligned}$$

where we used $\|\Delta_j\|_F = \sqrt{du} \sin(\theta)$ on the last line. Let $S := \sum_{i=1}^m \sum_{j=1}^{i-1} p^{m-j-1} = \sum_{i=1}^{m-1} ip^{i-1}$. Using a telescoping expansion leads to

$$\begin{aligned} S - pS &= -(m-1)p^{m-1} + \sum_{i=0}^{m-2} p^i \\ &= \frac{1-p^{m-1}}{1-p} - (m-1)p^{m-1} \\ \Rightarrow S &= \frac{1-mp^{m-1} - (m-1)p^m}{(1-p)^2} . \quad (\text{A12}) \end{aligned}$$

S is maximized when $p = 1$, in which case it equals $\binom{m}{2}$. □

-
- [1] J. P. Gaebler, A. M. Meier, T. R. Tan, R. Bowler, Y. Lin, D. Hanneke, J. D. Jost, J. P. Home, E. Knill, D. Leibfried, and D. J. Wineland, *Physical Review Letters* **108**, 260503 (2012).
- [2] A. D. Córcoles, J. M. Gambetta, J. M. Chow, J. A. Smolin, M. Ware, J. Strand, B. L. T. Plourde, and M. Steffen, *Physical Review A* **87**, 030301 (2013).
- [3] J. Kelly, R. Barends, B. Campbell, Y. Chen, Z. Chen, B. Chiaro, A. Dunsworth, A. G. Fowler, I.-C. Hoi, E. Jeffrey, A. Megrant, J. Mutus, C. Neill, P. J. J. O'Malley, C. Quintana, P. Roushan, D. Sank, A. Vainsencher, J. Wenner, T. C. White, A. N. Cleland, and J. M. Martinis, *Physical Review Letters* **112**, 240504 (2014), arXiv:1403.0035 [quant-ph].
- [4] R. Barends, J. Kelly, A. Megrant, A. Veitia, D. Sank, E. Jeffrey, T. C. White, J. Mutus, A. G. Fowler, B. Campbell, Y. Chen, Z. Chen, B. Chiaro, A. Dunsworth, C. Neill, P. O'Malley, P. Roushan, A. Vainsencher, J. Wenner, A. N. Korotkov, A. N. Cleland, and J. M. Martinis, *Nature* **508**, 500 (2014), letter.
- [5] T. Xia, M. Lichtman, K. Maller, A. W. Carr, M. J. Piotrowicz, L. Isenhower, and M. Saffman, *Phys. Rev. Lett.* **114**, 100503 (2015), arXiv:1501.02041 [quant-ph].
- [6] J. T. Muhonen, A. Laucht, S. Simmons, J. P. Dehollain, R. Kalra, F. E. Hudson, S. Freer, K. M. Itoh, D. N. Jamieson, J. C. McCallum, A. S. Dzurak, and A. Morello, *Journal of Physics: Condensed Matter* **27**, 154205 (2015).
- [7] J. E. Tarlton, *Probing qubit memory errors at the 10- 5 level*, Ph.D. thesis.
- [8] L. Casparis, T. W. Larsen, M. S. Olsen, F. Kuemmeth, P. Krogstrup, J. Nygård, K. D. Petersson, and C. M. Marcus, *Phys. Rev. Lett.* **116**, 150505 (2016).
- [9] D. C. McKay, S. Filipp, A. Mezzacapo, E. Magesan, J. M. Chow, and J. M. Gambetta, *Physical Review Applied* **6**, 064007 (2016).

- [10] S. Sheldon, E. Magesan, J. M. Chow, and J. M. Gambetta, *Physical Review A* **93**, 060302 (2016).
- [11] M. Takita, A. D. Córcoles, E. Magesan, B. Abdo, M. Brink, A. Cross, J. M. Chow, and J. M. Gambetta, *Phys. Rev. Lett.* **117**, 210505 (2016).
- [12] D. C. McKay, S. Sheldon, J. A. Smolin, J. M. Chow, and J. M. Gambetta, *ArXiv e-prints*, arXiv:1712.06550 (2017), arXiv:1712.06550 [quant-ph].
- [13] J. Emerson, R. Alicki, and K. Życzkowski, *Journal of Optics B: Quantum and Semiclassical Optics* **7**, S347 (2005).
- [14] C. Dankert, R. Cleve, J. Emerson, and E. Livine, *Phys. Rev. A* **80** (2009); arxiv.org/abs/quant-ph/0606161 (2006).
- [15] E. Magesan, J. M. Gambetta, and J. Emerson, *Physical Review Letters* **106**, 180504 (2011).
- [16] E. Magesan, J. M. Gambetta, B. R. Johnson, C. A. Ryan, J. M. Chow, S. T. Merkel, M. P. da Silva, G. A. Keefe, M. B. Rothwell, T. A. Ohki, M. B. Ketchen, and M. Steffen, *Physical Review Letters* **109**, 080505 (2012), arXiv:1203.4550.
- [17] J. Wallman, C. Granade, R. Harper, and S. T. Flammia, *New Journal of Physics* **17**, 113020 (2015).
- [18] J. J. Wallman, M. Barnhill, and J. Emerson, *Physical Review Letters* **115**, 060501 (2015).
- [19] J. J. Wallman and J. Emerson, *Physical Review A* **94**, 052325 (2016).
- [20] T. Proctor, K. Rudinger, K. Young, M. Sarovar, and R. Blume-Kohout, *Phys. Rev. Lett.* **119**, 130502 (2017).
- [21] J. J. Wallman, *Quantum* **2**, 47 (2018).
- [22] A. Carignan-Dugas, K. Boone, J. J. Wallman, and J. Emerson, *New Journal of Physics* **20**, 092001 (2018).
- [23] R. Harper, I. Hincks, C. Ferrie, S. T. Flammia, and J. J. Wallman, *arXiv e-prints*, arXiv:1901.00535 (2019), arXiv:1901.00535 [quant-ph].
- [24] B. Dirkse, J. Helsen, and S. Wehner, *Physical Review A* **99**, 012315 (2019), arXiv:1808.00850 [quant-ph].
- [25] S. T. Merkel, E. J. Pritchett, and B. H. Fong, *arXiv e-prints*, arXiv:1804.05951 (2018), arXiv:1804.05951 [quant-ph].
- [26] T. Proctor, K. Rudinger, K. Young, M. Sarovar, and R. Blume-Kohout, *arXiv e-prints*, arXiv:1702.01853v1 (2017), arXiv:1702.01853v1 [quant-ph].
- [27] J. Qi and H. Khoon Ng, *arXiv e-prints*, arXiv:1805.10622 (2018), arXiv:1805.10622 [quant-ph].
- [28] M. Veldhorst, J. C. C. Hwang, C. H. Yang, A. W. Leenstra, B. de Ronde, J. P. Dehollain, J. T. Muhonen, F. E. Hudson, K. M. Itoh, A. Morello, and A. S. Dzurak, *Nature Nanotechnology* **9**, 981 (2014), arXiv:1407.1950 [cond-mat.mes-hall].
- [29] M. Veldhorst, R. Ruskov, C. H. Yang, J. C. C. Hwang, F. E. Hudson, M. E. Flatté, C. Tahan, K. M. Itoh, A. Morello, and A. S. Dzurak, *Physical Review B* **92**, 201401 (2015), arXiv:1505.01213 [cond-mat.mes-hall].
- [30] R. Barends, L. Lamata, J. Kelly, L. García-Álvarez, A. G. Fowler, A. Megrant, E. Jeffrey, T. C. White, D. Sank, J. Y. Mutus, B. Campbell, Y. Chen, Z. Chen, B. Chiaro, A. Dunsworth, I. C. Hoi, C. Neill, P. J. J. O’Malley, C. Quintana, P. Roushan, A. Vainsencher, J. Wenner, E. Solano, and J. M. Martinis, *Nature Communications* **6**, 7654 (2015), arXiv:1501.07703 [quant-ph].
- [31] K. Takeda, J. Kamioka, T. Otsuka, J. Yoneda, T. Nakajima, M. R. Delbecq, S. Amaha, G. Allison, T. Koder, S. Oda, and S. Tarucha, *Science Advances* **2**, e1600694 (2016), arXiv:1602.07833 [cond-mat.mes-hall].
- [32] D. C. McKay, C. J. Wood, S. Sheldon, J. M. Chow, and J. M. Gambetta, *Physical Review A* **96**, 022330 (2017), arXiv:1612.00858 [quant-ph].
- [33] J. M. Nichol, L. A. Orona, S. P. Harvey, S. Fallahi, G. C. Gardner, M. J. Manfra, and A. Yacoby, *npj Quantum Information* **3**, 3 (2017), arXiv:1608.04258 [cond-mat.mes-hall].
- [34] K. W. Chan, W. Huang, C. H. Yang, J. C. C. Hwang, B. Hensen, T. Tanttu, F. E. Hudson, K. M. Itoh, A. Laucht, A. Morello, and A. S. Dzurak, *Physical Review Applied* **10**, 044017 (2018), arXiv:1803.01609 [quant-ph].
- [35] S. A. Caldwell, N. Didier, C. A. Ryan, E. A. Sete, A. Hudson, P. Karalekas, R. Manenti, M. P. da Silva, R. Sinclair, E. Acala, N. Alidoust, J. Angeles, A. Bestwick, M. Block, B. Bloom, A. Bradley, C. Bui, L. Capelluto, R. Chilcott, J. Cordova, G. Crossman, M. Curtis, S. Deshpande, T. E. Bouayadi, D. Girshovich, S. Hong, K. Kuang, M. Lenihan, T. Manning, A. Marchenkov, J. Marshall, R. Maydra, Y. Mohan, W. O’Brien, C. Osborn, J. Otterbach, A. Papageorge, J. P. Paquette, M. Pelstring, A. Polloreno, G. Prawiroatmodjo, V. Rawat, M. Reagor, R. Renzas, N. Rubin, D. Russell, M. Rust, D. Scarabelli, M. Scheer, M. Selvanayagam, R. Smith, A. Staley, M. Suska, N. Tezak, D. C. Thompson, T. W. To, M. Vahidpour, N. Vdrahalli, T. Whyland, K. Yadav, W. Zeng, and C. Rigetti, *Physical Review Applied* **10**, 034050 (2018), arXiv:1706.06562 [quant-ph].
- [36] T. Wang, Z. Zhang, L. Xiang, Z. Jia, P. Duan, W. Cai, Z. Gong, Z. Zong, M. Wu, J. Wu, L. Sun, Y. Yin, and G. Guo, *New Journal of Physics* **20**, 065003 (2018), arXiv:1804.08247 [quant-ph].
- [37] T. Wang, Z. Zhang, L. Xiang, Z. Jia, P. Duan, Z. Zong, Z. Sun, Z. Dong, J. Wu, Y. Yin, and G. Guo, *arXiv e-prints*, arXiv:1811.08096 (2018), arXiv:1811.08096 [quant-ph].
- [38] J. Yoneda, K. Takeda, T. Otsuka, T. Nakajima, M. R. Delbecq, G. Allison, T. Honda, T. Koder, S. Oda, Y. Hoshi, N. Usami, K. M. Itoh, and S. Tarucha, *Nature Nanotechnology* **13**, 102 (2018), arXiv:1708.01454 [cond-mat.mes-hall].
- [39] Z. Zhang, P. Z. Zhao, T. Wang, L. Xiang, Z. Jia, P. Duan, D. M. Tong, Y. Yin, and G. Guo, *arXiv e-prints*, arXiv:1811.06252 (2018), arXiv:1811.06252 [quant-ph].
- [40] A. Carignan-Dugas, J. J. Wallman, and J. Emerson, *Physical Review A* **92**, 060302 (2015), arXiv:1508.06312 [quant-ph].
- [41] A. W. Cross, E. Magesan, L. S. Bishop, J. A. Smolin, and J. M. Gambetta, *npj Quantum Information* **2**, 16012 (2016), arXiv:1510.02720 [quant-ph].
- [42] R. Harper and S. T. Flammia, *Quantum Science and Technology* **2**, 015008 (2017), arXiv:1608.02943 [quant-ph].
- [43] T. J. Proctor, A. Carignan-Dugas, K. Rudinger, E. Nielsen, R. Blume-Kohout, and K. Young, *arXiv e-prints*, arXiv:1807.07975 (2018), arXiv:1807.07975 [quant-ph].
- [44] A. Carignan-Dugas, Extended analysis of RB-type protocols under gate-dependent noise models (Upcoming work).
- [45] X. Xue, T. F. Watson, J. Helsen, D. R. Ward, D. E. Savage, M. G. Lagally, S. N. Coppersmith, M. A. Eriksson, S. Wehner,

- and L. M. K. Vandersypen, arXiv e-prints , arXiv:1811.04002 (2018), arXiv:1811.04002 [quant-ph].
- [46] C. H. Yang, K. W. Chan, R. Harper, W. Huang, T. Evans, J. C. C. Hwang, B. Hensen, A. Laucht, T. Tanttu, F. E. Hudson, S. T. Flammia, K. M. Itoh, A. Morello, S. D. Bartlett, and A. S. Dzurak, arXiv e-prints , arXiv:1807.09500 (2018), arXiv:1807.09500 [cond-mat.mes-hall].
- [47] S. Kimmel, M. P. da Silva, C. a. Ryan, B. R. Johnson, and T. a. Ohki, Physical Review X **4**, 011050 (2014).
- [48] D. Pérez-García, M. M. Wolf, D. Petz, and M. B. Ruskai, Journal of Mathematical Physics **47**, 083506 (2006), math-ph/0601063.
- [49] R. Bhatia, *Matrix Analysis* (Springer, 1997).